Eur. Phys. J. D (2022) 76:85
https://doi.org/10.1140/epjd/s10053-022-00404-8

THE EUROPEAN PHYSICAL JOURNAL D

Regular Article - Ultraintense and Ultrashort Laser Fields

Optimization of high-order harmonic generation for the time-resolved ARPES

Yueying Liang[1,3], Xinkui He[1,3,4,a], Liqiang Liu[2], Junli Wang[2], Shuai Wang[1,3], and Zhiyi Wei[1,2,3,b]

[1] Beijing National Laboratory for Condensed Matter Physics, Institute of Physics, Chinese Academy of Sciences, Beijing 100190, People's Republic of China
[2] School of Physics and Optoelectronic Engineering, Xidian University, Xi'an 710071, People's Republic of China
[3] University of Chinese Academy of Science, Beijing 10049, People's Republic of China
[4] Songshan Lake Materials Laboratory, Dongguan 523808, Guangdong, People's Republic of China

Received 7 February 2022 / Accepted 18 April 2022 / Published online 16 May 2022

Abstract. We experimentally investigated the optimized phase matching condition for high order harmonic generation as a source of time-resolved Angle-resolved photoemission spectroscopy (TR-ARPES) applications. In the loose focusing scheme, we find that the divergence of harmonics decreases with the increase of gas cell length, while the maximum intensity is obtained with 10–15 mm gas cell. Our result shows that stable beam condition with best temporal resolution can be realized for TR-ARPES by using a longer gas cell (longer than 25 mm in our experiment), and an appropriate gas cell length can provide balanced condition for good beam intensity and good temporal resolution.

Over the past 20 years, high-order harmonic has become an important source for extreme ultraviolet (XUV) radiation [1, 2]. High-order harmonic is normally generated by the interaction between an intense laser and noble gas. Compared to the other generation methods of XUV sources, such as X-ray free-electrons lasers (XFELs) and soft X-ray lasers (SXRLs), high-order harmonic has the unique features of high temporal and spatial coherence, high temporal resolution as well as tabletop scale. Therefore, it is widely used in the study of the atomic and molecular spectroscopy [3, 4], the time-resolved photoemission electron microscopy (TR-PEEM) [5] and the XUV holography [6, 7].

Angle-resolved photoemission spectroscopy (ARPES) is a powerful experimental technique for probing the electronic band structure of solid materials. Based on the photoelectric effect, the energy–momentum dispersion relationship is detected by measuring the energy and momentum of the photoelectrons ejected by incident photons [8], which is normally in XUV range and from traditional sources like noble gas discharge lamp [9, 10]or synchrotron radiation [11–13]. The measurement of the band structure using these sources is limited to the equilibrium state in solids. With the development of femtosecond lasers, the light sources based on nonlinear optical processes are also applied in ARPES experiments, such as second harmonic generation [14, 15] and four-wave mixing [16]. The ultrafast laser source combined with ARPES can provide not only higher energy and momentum resolution [17] but also high temporal resolution. It is becoming possible to study the excitation process of electrons. However, visible and ultraviolet wavelength severely limit its application. In recent years, high-order harmonics with the photon energy of tens of electron volt in a wide spectral range and ultrafast time scale gradually become the new promising source for time-resolved ARPES (TR-ARPES). Using this powerful scientific instrument, some important experiments to detect the electron dynamics with the ultrafast time scale have been carried out, such as the out-of-equilibrium dynamics of quantum materials [18, 19], the hot carrier dynamics in grapheme [20] and so on. The typical time resolution is as short as sub-100 fs with the energy resolution of hundreds of meV [18, 20–22].

Radiation from high order harmonic generation usually has a wide spectral range in the EUV regime with a discrete spectrum consist of odd harmonic of fundamental laser. For TR-ARPES, a monochromator is necessary to select a narrow bandwidth from the harmonic spectrum. A typical monochromator for high-order harmonics usually consists of two toroidal mirror and a grating [23]. The harmonic is firstly collimated by a toroidal mirror, then spatially separated with different diffraction angles by the grating, and finally focused by the second toroidal mirror to a slit vertical to the direction of grating grooves to select the specific wavelength. By rotating the grating, different wavelength of the harmonics with narrow bandwidth can be selected.

[a] e-mail: xinkuihe@iphy.ac.cn (corresponding author)
[b] e-mail: zywei@iphy.ac.cn (corresponding author)

However, the selection of photon energy using reflection grating has an inevitable side effect, which is the broadening of the pulse from wavefront tilt. For the first order diffraction, the delay between two rays reflected by the adjacent grooves is one wavelength. The total delay of the whole beam is $N\lambda$, where N is the number of illuminated grooves, λ is the wavelength of the laser. For a harmonic with wavelength of 40 nm diffracted by a 100 gr/mm grating, for the increase of the illumined area of each 10 mm, the increase of time delay will be 133 fs, which is too big for TR-ARPES measurement. Although another grating can be used to compensate the wavefront tilt [24–27], the total efficiency of the monochromator will be substantially decreased, which is already very low even in one grating configuration. Therefore, monochromator for selecting narrow band source from harmonic usually uses one grating configuration.

Using monochromator in TR-ARPES brings specific demands for high-order harmonic generation. The harmonic source must be optimized to a balance between high intensity and low divergence to decrease the illuminated area on the grating and at the same time have enough photons for ARPES [23]. Furthermore, the high intensity and low divergence must be fulfilled in a wide spectral range since the ARPES measurement often needs a wavelength scan. The experimental condition in the generation of high-order harmonics, including gas cell length, gas pressure, gas cell position also needs to be stable and without additional adjustment during the wavelength scan to ensure a stable measurement and to keep a reasonable measurement time.

Since the intensity and divergence of harmonic origin from the generation process, many works have been done to improve the phase matching condition. For example, the waveguide geometry is used for balancing the phase-mismatch from the medium and the waveguide [28, 29]. The loose focusing geometry combined with long gas cell is applied to decrease the radially variation of harmonic phase, for the generation of harmonics with low divergence [30, 31]. The use of truncated Bessel beam is investigated to flatten the total harmonic phase front for a collimated beam generation in a thin gas medium [32]. Recently, the two-color orthogonally polarized laser field is introduced to select one trajectory to control the harmonic divergence [33]. Although some measurement have been taken to investigate HHG under the influences of gas pressure and focal position [34], because of the specific demands for ARPES application, a systematic discussion of the phase matching condition for high order harmonic generation is still necessary.

In this paper, we investigate the variation of the harmonic intensity and divergence at different phase matching condition experimentally. Our result shows that by optimizing the phase matching condition of HHG, including the gas cell length, gas pressure and the position of the gas cell relative to the laser focus, it is possible to obtain the XUV beam with the suitable photon flux and low divergence in a relatively wide spectral range. The result is helpful for the further applications of harmonics on Tr-APRES.

The laser used in our experiment is a homemade Ti: sapphire laser with the repetition rate of 1 kHz and the pulse duration of 40 fs. The central wavelength is 800 nm. An aperture is put in the beam to optimize the beam quality as well as adjust the intensity at the laser focus. The beam diameter after the aperture is around 10 mm, corresponding to the pulse energy of 12 mJ. The laser is focused by a concave mirror with the focal length of 1.5 m into a pulsed gas cell with the same repetition rate of 1 kHz. Argon is used in the experiment and the relative delay between the laser pulse and the gas pulse can be adjusted. A homemade flat-field spectrometer consisting of a grating and microchannel plate (MCP) is used for measuring the spatial-frequency distribution of the harmonics. The intensity of harmonics imaging on MCP is recoded by a charge-coupled device (CCD) camera. The distance between the generation position and the MCP is 2 m.

A typical spatial-frequency distribution of harmonics generated by 25 mm gas cell is shown in Fig. 1a. Harmonics from 19th up to 41st are observed, corresponding to the photon energy from 29 to 63 eV. In our experiment, after the generation, the harmonics are directly cut by a slit, then dispersed by the grating and finally collected by the MCP without any focusing device. Therefore, the divergence and intensity distribution of harmonics are directly measured without any distortion. To optimize the high-order harmonics to fulfill the demands of the TR-ARPES, gas target with different length, different pressure and different position relative to the focus of the laser beam is investigated. The minimum gas cell length is 2 mm, and then adjusted from 5 to 30 mm with the step of 5 mm. The diameter of the pinhole on the gas cell is 1 mm. To obtain a harmonic beam with good intensity and good beam quality, the gas pressure is optimized for each length of gas cell, which is shown in Fig. 1b. The dotted line shows the fitted curve of the relationship between the gas cell length and the optimized gas pressure. The optimized gas pressure is almost linearly decreased with the increase of the gas cell length. For a fixed gas cell length and pressure, the gas cell position is scanned from − 30 mm to 30 mm relative to the laser focus with a step of 10 mm in the direction along the laser propagation, to optimize the intensity of harmonics.

To investigate the optimized condition for TR-ARPES, the integrated intensity of the 27th harmonic as a function of the gas cell position for different gas cell length is shown in Fig. 2a. The integrated intensity is defined as the sum of the harmonics intensities of each pixels detected on the CCD. It can be find that the optimized intensity of harmonic changes quite a lot with the variation of the medium length. The intensity increases with the increase of gas cell length, and reaches the maximum when 10 mm gas cell is used. Then it decreases using the gas cell length longer than 10 mm. For the 30 mm case, the intensity of harmonic is lower than the case of 2 mm at the optimized gas pressure and gas cell position. For each length of gas

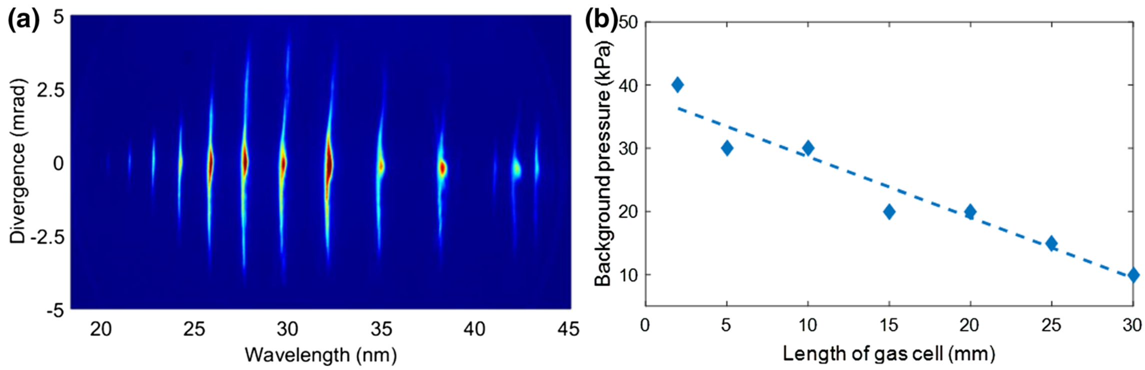

Fig. 1 **a** The measured spatial-frequency distribution of high order harmonics generated using 25 mm gas cell at the laser focus. **b** The optimized gas pressures for the perfect phase matching condition of different lengths of gas cell

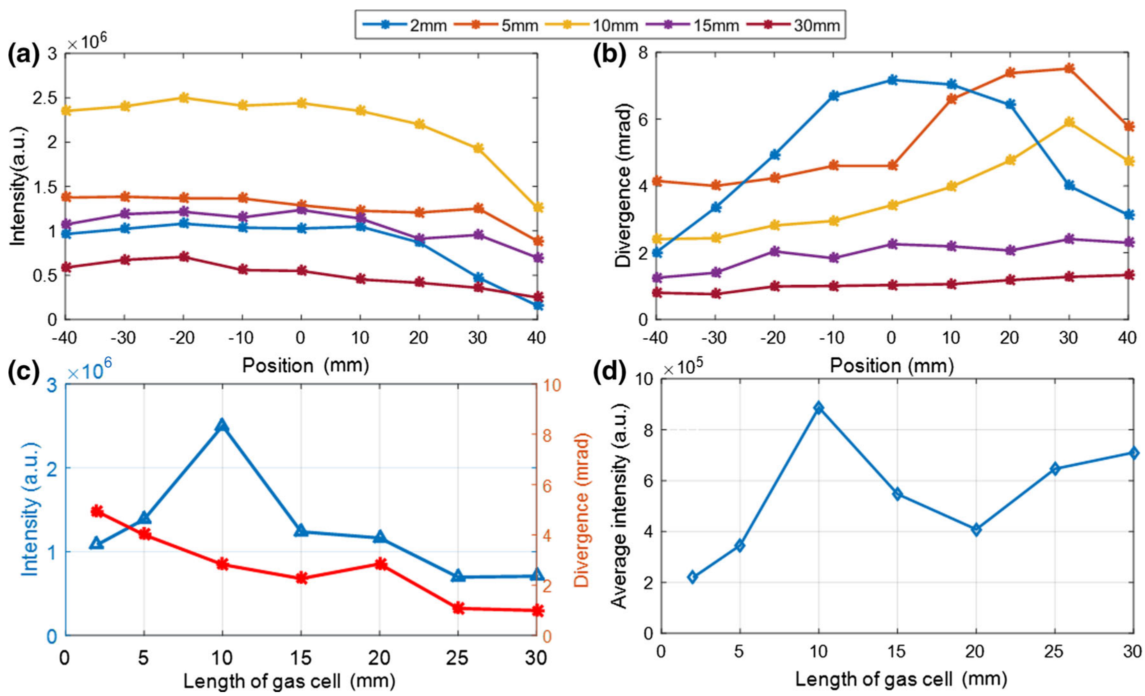

Fig. 2 The integrated intensity **a** and the divergence **b** of 27th harmonics as a function of the gas cell position relative to the laser focus using different lengths of gas cell. The focus is at z = 0 mm, and the negative value means the positions before laser focus. **c** The maximum intensity (blue line) and the corresponding divergence (red line) of 27th harmonic generated by different length of gas cell. **b** The intensity of the 27th harmonic per unit area

cells, the intensity of harmonic changes slowly with the variation of gas cell position. The intensity decreases when the gas cell is set at more than 20 mm behind the laser focus, and the decrease is larger for the 10 mm gas cell compared with other gas cell length. Our result shows that the harmonic intensity is enhanced using the 10 mm gas cell at the optimized phase matching condition, and which is not very sensitive to the location of gas cell.

The divergence of the harmonic can be calculated by the ratio between the full width at half minimum (FWHM) of the harmonic radial length detected at MCP to the distance of the laser focus and the MCP position. The divergence of the 27th harmonic as a function of gas cell length and gas cell position is shown in Fig. 2b. One can easily find that the divergence of the harmonic changes a lot with both the gas cell length and position. It decreases significantly with the increase of gas cell length. For the shortest 2 mm gas cell length, the divergence decreases quickly with the increase of the distance between the gas cell position and laser focus. The maximum divergence at the laser focus is almost twice to the case when the gas cell is positioned at 30 mm. With the increase of the gas cell length, the maximum divergence position moves in the direction of the laser propagation, and is not very sensitive to the position any more for the gas cell longer than 15 mm.

For the 30 mm gas cell, the divergence of harmonics generated in the whole measurement range is almost the same, which is less than 1 mrad and only 1/7 of the maximum divergence for 2 mm gas cell.

Figure 2c shows more detailed result of the maximum intensity for each length of gas cell and the corresponding divergence as a function of gas cell length for 27th harmonic. Obviously the best harmonic intensity is obtained by 10 mm gas cell, and it continuously decreases with the increase of the cell length. The divergence also keeps decreasing. This decrease gradually slows down and remains almost unchanged for the gas cell longer than 25 mm. For the experiments with high time resolution and low requirement of photon flux, the gas cell longer than 25 mm is a good choice for the low-divergence harmonic generation. On the contrary, the harmonic with high photon flux and relatively high divergence generated by 10 mm gas cell is suitable for the experiments demanding low time resolution and high photon flux. For the same harmonic intensity, compared to the harmonics generated by the gas cell shorter than 10 mm, the harmonics generated by the longer gas cell is much better for the applications of TR-ARPES. The balance of the divergence and intensity of harmonics can be achieved using 15 mm gas cell.

To understand the results obtained in the experiment, the coherent length for the long and short trajectory for gas target putting at different position relative to laser focus is investigated. The space-dependent coherent length can be written as $L_{q,coh}(r,z) = \frac{\pi}{|\delta \boldsymbol{k}(r,z)|}$. $\delta \boldsymbol{k}(r,z)$ is the wave vector mismatch of the harmonic and the fundamental laser, which is defined as $\delta \boldsymbol{k}(r,z) = \boldsymbol{k_q} - |\mathrm{q}\boldsymbol{k}_1 + \boldsymbol{K}|$ [35, 36]. Here $\boldsymbol{k_q}$ is the wave vector of the qth harmonic and $\boldsymbol{k}_1$ is the wave vector of the fundamental Gaussian beam, which comes from the phase different of harmonics and fundamental laser [37, 38]. $\boldsymbol{K}$ is the gradient of the atomic phase calculated by $\boldsymbol{K} = \nabla \Phi_{at}$. In our simulation, the atomic phase is supposed to be linearly dependent on the laser intensity $\boldsymbol{I}_0$ approximately, $\Phi_{at} = \alpha \boldsymbol{I}_0$. The coefficient α for the short and long trajectory is calculated using the strong field approximation (SFA) model.

The calculated coherent length of the 27th harmonic as a function of generation position for the short and long trajectories is shown in Fig. 3. For the short trajectory, the coherent length does not change much with the generation position, as the contribution from the dipole phase is quite small. For the harmonics generated from − 40 mm to 30 mm, both on-axis and off-axis, the coherent length is around 10 mm. This fits quite well with our experiment. When the gas cell much shorter than 10 mm is used, the coherent length is much longer than the media length. The number of gas atoms increases at high gas pressure, enhancing the output harmonic intensity. For the long trajectory, the region of the perfect phase matching is very sensitive to the location of the gas atom. The harmonics generated from 5 to 20 mm after the laser focus are well phase-matched on axis. In this region, the direction of **k** and **K** are the same and **K** compensate the phase-mismatch due to the laser geometry. The harmonics generated before the laser focus are phase-matched only off-axis because of the large gradient of the dipole phase. For the harmonics generated before laser focus, only the short trajectory is well phase-matched. The long trajectory is phase-matched off-axis and the corresponding electric field at this region is quite small. Thus, the divergence of harmonics is mainly contributed by the short trajectory. For the harmonics generated near the laser focus, the phase matching region for the long trajectory moves from off-axis to on-axis. The large change of the divergence of long trajectory is involved in the divergence of the total harmonic generation, corresponding to the divergence change in Fig. 2b of the 2 mm case.

With the increase of gas cell length, in order to decrease the absorption effect as well as the dispersion to the fundamental laser, the optimized gas pressure decreases. The optimized length of gas medium is 10 mm for the maximum harmonic generation. As the wave vector of harmonics in the off-axis region is not parallel to the laser propagation direction, it is difficult for the off-axis harmonics to achieve the perfect phase matching in the long gas medium. For the long gas cell, only the harmonics generated around the axis of the short trajectory are enhanced continuously, which lead to the decrease of the divergence. Our result also indicates that the short gas cell is sensitive to the phase matching condition, while the long gas cell shows more features of propagation effect.

To fulfill the demand of keeping stable generation condition and similar beam property for TR-ARPES, we have investigated the order-dependent maximum intensity and the corresponding divergence as a function of gas cell length, which is shown in Fig. 4. For the 25th, 29th, 33rd and 39th harmonics, 10 mm is also the best gas cell length for intensity. Although there are some fluctuations of intensity due to the energy fluctuation of the fundamental laser, the overall trend is that the integrated intensity increases with the increase of the gas cell length from 2 to 10 mm, and decrease as the gas cell further increases to 30 mm. For the harmonics of low order, the intensity increases more rapidly with the increase of the gas cell length than that of high order. For a fixed length of gas cell, the intensity decreases with the increase of harmonic order, as the efficiency of harmonic generation in single atom level decreases with the photon energy and the phase-mismatch introduced by the dipole phase is also larger for the harmonics with high photon energy.

The beam divergence of the 25th, 29th, 33rd and 39th harmonics shown in Fig. 4b decreases with the increase of gas cell length, which is similar to the behavior of 27th. The result shows that it is effective to obtain a harmonic beam with low divergence using a long gas cell. For a given gas cell length, the divergence of harmonic beam shows a decreasing trend with the increase of photon energy. This is also due to the large phase-mismatch of the off-axis part introduced the dipole phase for the high harmonics with high photon energy.

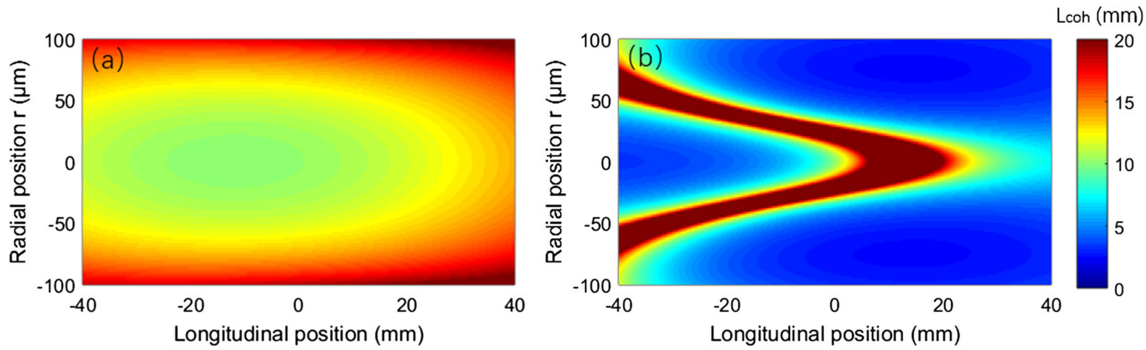

Fig. 3 **a** The average intensity obtained with the optimized gas cell length for each harmonic order. **b** The corresponding optimized gas cell position

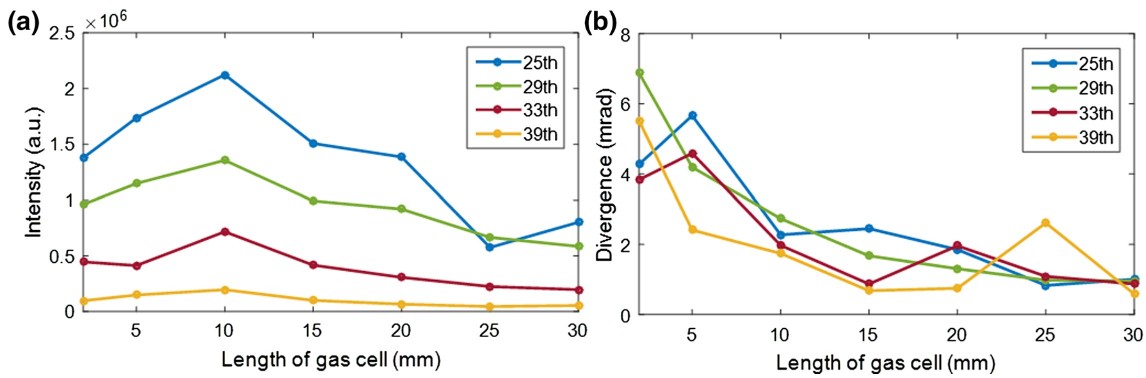

Fig. 4 The maximum integrated intensity (**a**) and the corresponding divergence (**b**) of 25th (blue line), 29th (green line), 33rd (red line) and 39th (yellow line) harmonics for each length of gas cell

The result indicates that although the change of harmonics between the different orders are determined by the phase matching condition, the variation of intensity and divergence as a function of gas cell length and position are quite similar in a wide spectral range of harmonics. If the harmonic intensity is not an important issue, using a long gas cell (longer than 25 mm in our case) is a promising method for minimizing the wavefront tilt and obtaining the best temporal resolution in TR-ARPES experiment. If the decrease of the harmonic intensity for long gas cell is not acceptable in the experiment, then an appropriate gas cell to balance the harmonic intensity and the beam divergence should be used.

To find the balanced harmonic generation condition for TR-ARPES experiment, we calculate the harmonic intensity per unit area, which is defined as $i = \frac{I}{l*d}$. Here I is the integrated intensity defined above, l is the FWHM of the harmonic radial length on the MCP and d is the width of the silt. For the 27th harmonic, i increases with the increase of gas cell length, and reaches maximum for the 10 mm gas cell, which is shown in Fig. 2d. This is because the decrease of the divergence is relatively slow compare with the increase of harmonic intensity, thus the maximum average intensity is still obtained by using 10 mm gas cell. The gas cell length, gas cell position and the corresponding maximum average intensity generation for harmonics from the 23rd to the 39th are shown in Fig. 5a, b. Despite the fluctuation appeared in the generation of 29th harmonic, the optimization of harmonics of low order and high order is obtained in a relatively stable generation condition. For the harmonics from 23rd to 27th, the optimized gas cell length is 10 mm, and the optimized gas cell position is 20 mm in front of the laser focus. For the harmonics of higher order from 31st to 39th, the optimized gas cell length is 15 mm and with an optimized position of 30 mm in front of the laser focus. The result shows that, by using a gas cell with appropriate length at the right position, a collimated beam with relative high energy in a wide spectral range can be obtained without adjustment of generation condition. For the spectrum from the 23rd to the 39th harmonic, the minimum divergence is 0.68 mrad, less than the typical divergence of 1–20 mrad [39–41] of the XUV beam used in Tr-ARPES. The photon flux is estimated to be above 10^7 phs/short, which is above the typical photon flux of 3.3×10^6phs/short [39] for Tr-ARPES. The photon flux can be adjusted by an aperture while the divergence can be further decreased, corresponding to a better time resolution. A stable and tunable source for the best temporal resolution of TR-ARPES can be realized.

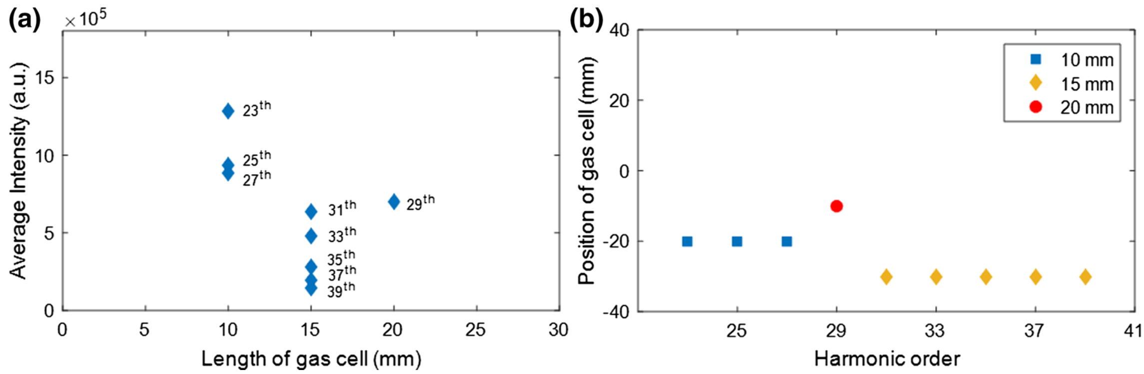

Fig. 5 **a** The maximum average intensity of each order and the corresponding length of gas cell. **b** The corresponding position of the gas cell for the maximum average intensity of each order

In conclusion, based on the demand of TR-ARPES experiment, we have experimentally investigated the intensity and beam divergence of high-order harmonics generated in Ar for different gas cell condition. The maximum intensity is achieved using 10 mm gas cell. When the length of the gas cell is longer than 10 mm, both the intensity and the beam divergence decrease with the increase of the gas cell length and are not sensitive to the gas cell position any more. This provides very stable parameter range for the TR-ARPES experiment pursuing the good temporal resolution. For the experiment concerns for both the photon flux and temporal resolution, parameter range for the balance between intensity and beam divergence must be used, which can be obtained using the gas cell around 10 mm and 15 mm and the result is effective in a wide spectral range. Our research shows that by optimizing the phase matching condition of HHG, including the gas cell length, gas pressure and the position of the gas cell relative to the laser focus, the XUV beam with both high flux and low divergence can be generated, which provides a promising light source for the TR-ARPES.

Acknowledgements The authors would like to thank Hao Teng and Kun Zhao for helpful discussions.

Author contributions

The idea was proposed by Xinkui He and Yueying Liang, and the results were done and analyzed by Yueying Liang and Liqiang Liu. All the authors have contributed to the final version of the manuscript.

Funding National Natural Science Foundation of China (11974416, 91850209).

Data availability statement Data underlying the results presented in this paper are not publicly available at this time but may be obtained from the authors upon reasonable request. "This manuscript has associated data in a data repository. [Authors' comment: Data is available from the corresponding author on reasonable request]".

Declarations

Conflict of interest The authors declare no conflicts of interest.

References

1. J.L. Krause, K.J. Schafer, K.C. Kulander, High-order harmonic generation from atoms and ions in the high intensity regime. Phys. Rev. Lett. **68**, 3535 (1992)
2. J.J. Macklin, J. Kmetec, C. Gordon III., High-order harmonic generation using intense femtosecond pulses. Phys. Rev. Lett. **70**, 766 (1993)
3. M. Bauer, C. Lei, K. Read, R. Tobey, J. Gland, M. Murnane, H. Kapteyn, Direct observation of surface chemistry using ultrafast soft-x-ray pulses. Phys. Rev. Lett. **87**, 025501 (2001)
4. L. Nugent-Glandorf, M. Scheer, D.A. Samuels, A.M. Mulhisen, E.R. Grant, X. Yang, V.M. Bierbaum, S.R. Leone, Ultrafast time-resolved soft x-ray photoelectron spectroscopy of dissociating Br 2. Phys. Rev. Lett. **87**, 193002 (2001)
5. E. Mårsell, C.L. Arnold, E. Lorek, D. Guenot, T. Fordell, M. Miranda, J. Mauritsson, H. Xu, A. L'Huillier, A. Mikkelsen, Secondary electron imaging of nanostructures using Extreme Ultra-Violet attosecond pulse trains and Infra-Red femtosecond pulses. Ann. Phys. **525**, 162–170 (2013)
6. R.A. Bartels, A. Paul, H. Green, H.C. Kapteyn, M.M. Murnane, S. Backus, I.P. Christov, Y. Liu, D. Attwood, C. Jacobsen, Generation of spatially coherent light at extreme ultraviolet wavelengths. Science **297**, 376–378 (2002)
7. D. Treacher, D. Lloyd, F. Wiegandt, K. O'Keeffe, S. Hooker, Optimised XUV holography using spatially shaped high harmonic beams. Opt. Express **27**, 29016–29025 (2019)
8. A. Damascelli, Probing the electronic structure of complex systems by ARPES. Phys. Scr. **2004**, 61 (2004)

9. S. He, J. He, W. Zhang, L. Zhao, D. Liu, X. Liu, D. Mou, Y.-B. Ou, Q.-Y. Wang, Z. Li, Phase diagram and electronic indication of high-temperature superconductivity at 65 K in single-layer FeSe films. Nat. Mater. **12**, 605–610 (2013)
10. Z.-H. Zhu, G. Levy, B. Ludbrook, C. Veenstra, J. Rosen, R. Comin, D. Wong, P. Dosanjh, A. Ubaldini, P. Syers, Rashba spin-splitting control at the surface of the topological insulator Bi 2 Se 3. Phys. Rev. Lett. **107**, 186405 (2011)
11. B. Lv, N. Xu, H. Weng, J. Ma, P. Richard, X. Huang, L. Zhao, G. Chen, C. Matt, F. Bisti, Observation of Weyl nodes in TaAs. Nat. Phys. **11**, 724–727 (2015)
12. Y. Saitoh, H. Kimura, Y. Suzuki, T. Nakatani, T. Matsushita, T. Muro, T. Miyahara, M. Fujisawa, K. Soda, S. Ueda, Performance of a very high resolution soft x-ray beamline BL25SU with a twin-helical undulator at SPring-8. Rev. Sci. Instrum. **71**, 3254–3259 (2000)
13. S.-Y. Xu, I. Belopolski, N. Alidoust, M. Neupane, G. Bian, C. Zhang, R. Sankar, G. Chang, Z. Yuan, C.-C. Lee, Discovery of a Weyl fermion semimetal and topological Fermi arcs. Science **349**, 613–617 (2015)
14. J. Koralek, J. Douglas, N. Plumb, J. Griffith, S. Cundiff, H. Kapteyn, M. Murnane, D. Dessau, Experimental setup for low-energy laser-based angle resolved photoemission spectroscopy. Rev. Sci. Instrum. **78**, 053905 (2007)
15. T. Kiss, T. Shimojima, K. Ishizaka, A. Chainani, T. Togashi, T. Kanai, X.-Y. Wang, C.-T. Chen, S. Watanabe, S. Shin, A versatile system for ultrahigh resolution, low temperature, and polarization dependent Laser-angle-resolved photoemission spectroscopy. Rev. Sci. Instrum. **79**, 023106 (2008)
16. F. Cilento, A. Crepaldi, G. Manzoni, A. Sterzi, M. Zacchigna, P. Bugnon, H. Berger, F. Parmigiani, Advancing non-equilibrium ARPES experiments by a 9.3 eV coherent ultrafast photon source. J. Electron Spectrosc. Relat. Phenom. **207**, 7–13 (2016)
17. E.J. Sie, XUV-Based Time-Resolved ARPES, in *Coherent Light-Matter Interactions in Monolayer Transition-Metal Dichalcogenides* (Springer, 2018), pp. 115–129.
18. I. Gierz, J.C. Petersen, M. Mitrano, C. Cacho, I.E. Turcu, E. Springate, A. Stöhr, A. Köhler, U. Starke, A. Cavalleri, Snapshots of non-equilibrium Dirac carrier distributions in graphene. Nat. Mater. **12**, 1119–1124 (2013)
19. R. Carley, K. Döbrich, B. Frietsch, C. Gahl, M. Teichmann, O. Schwarzkopf, P. Wernet, M. Weinelt, Femtosecond laser excitation drives ferromagnetic gadolinium out of magnetic equilibrium. Phys. Rev. Lett. **109**, 057401 (2012)
20. J.C. Johannsen, S. Ulstrup, F. Cilento, A. Crepaldi, M. Zacchigna, C. Cacho, I.E. Turcu, E. Springate, F. Fromm, C. Raidel, Direct view of hot carrier dynamics in graphene. Phys. Rev. Lett. **111**, 027403 (2013)
21. G. Rohde, A. Hendel, A. Stange, K. Hanff, L.-P. Oloff, L. Yang, K. Rossnagel, M. Bauer, Time-resolved ARPES with sub-15 fs temporal and near Fourier-limited spectral resolution. Rev. Sci. Instrum. **87**, 103102 (2016)
22. M. Hajlaoui, E. Papalazarou, J. Mauchain, Z. Jiang, I. Miotkowski, Y. Chen, A. Taleb-Ibrahimi, L. Perfetti, M. Marsi, Time resolved ultrafast ARPES for the study of topological insulators: The case of Bi 2 Te 3. European Phys. J. Spec. Top. **222**, 1271–1275 (2013)
23. F. Frassetto, C. Cacho, C.A. Froud, I.E. Turcu, P. Villoresi, W.A. Bryan, E. Springate, L. Poletto, Single-grating monochromator for extreme-ultraviolet ultrashort pulses. Opt. Express **19**, 19169–19181 (2011)
24. L. Poletto, P. Villoresi, F. Frassetto, F. Calegari, F. Ferrari, M. Lucchini, G. Sansone, M. Nisoli, Time-delay compensated monochromator for the spectral selection of extreme-ultraviolet high-order laser harmonics. Rev. Sci. Instrum. **80**, 123109 (2009)
25. G. Dakovski, Y. Li, T. Durakiewicz, G. Rodriguez, Tunable ultrafast extreme ultraviolet source for time-and angle-resolved photoemission spectroscopy. Rev. Sci. Instrum. **81**, 073108 (2010)
26. H. Igarashi, A. Makida, M. Ito, T. Sekikawa, Pulse compression of phase-matched high harmonic pulses from a time-delay compensated monochromator. Opt. Express **20**, 3725–3732 (2012)
27. M. Eckstein, J. Hummert, M. Kubin, C.-H. Yang, F. Frassetto, L. Poletto, M. J. Vrakking, and O. Kornilov, Alignment and characterization of the two-stage time delay compensating XUV monochromator, arXiv preprint arXiv:1604.02650 (2016).
28. T. Popmintchev, M.-C. Chen, A. Bahabad, M. Gerrity, P. Sidorenko, O. Cohen, I.P. Christov, M.M. Murnane, H.C. Kapteyn, Phase matching of high harmonic generation in the soft and hard X-ray regions of the spectrum. Proc. Natl. Acad. Sci. **106**, 10516–10521 (2009)
29. A. Rundquist, C.G. Durfee, Z. Chang, C. Herne, S. Backus, M.M. Murnane, H.C. Kapteyn, Phase-matched generation of coherent soft X-rays. Science **280**, 1412–1415 (1998)
30. D. Lee, H. Kim, K. Hong, C.H. Nam, I. Choi, A. Bartnik, H. Fiedorowicz, Generation of bright low-divergence high-order harmonics in a long gas jet. Appl. Phys. Lett. **81**, 3726–3728 (2002)
31. E.J. Takahashi, Y. Nabekawa, K. Midorikawa, Low-divergence coherent soft x-ray source at 13 nm by high-order harmonics. Appl. Phys. Lett. **84**, 4–6 (2004)
32. P. Ye, H. Teng, X.-K. He, S.-Y. Zhong, L.-F. Wang, M.-J. Zhan, W. Zhang, C.-X. Yun, Z.-Y. Wei, Minimizing the angular divergence of high-order harmonics by truncating the truncated Bessel beam. Phys. Rev. A **90**, 063808 (2014)
33. S.R. Abbing, F. Campi, F.S. Sajjadian, N. Lin, P. Smorenburg, P.M. Kraus, Divergence control of high-harmonic generation. Phys. Rev. Appl. **13**, 054029 (2020)
34. J. Yao, H. Xiong, H. Xu, Y. Fu, B. Zeng, W. Chu, Y. Cheng, Z. Xu, X. Liu, J. Chen, A systematic investigation of high harmonic generation using mid-infrared driving laser pulses. Sci. China Phys., Mech. Astron. **53**, 1054–1059 (2010)
35. P. Balcou, P. Salieres, A. L'Huillier, M. Lewenstein, Generalized phase-matching conditions for high harmonics: The role of field-gradient forces. Phys. Rev. A **55**, 3204 (1997)
36. L. Chipperfield, P. Knight, J. Tisch, J. Marangos, Tracking individual electron trajectories in a high harmonic spectrum. Opt. Commun. **264**, 494–501 (2006)

37. P. Salieres, A. L'Huillier, M. Lewenstein, Coherence control of high-order harmonics. Phys. Rev. Lett. **74**, 3776 (1995)
38. F. Lindner, G.G. Paulus, H. Walther, A. Baltuška, E. Goulielmakis, M. Lezius, F. Krausz, Gouy phase shift for few-cycle laser pulses. Phys. Rev. Lett. **92**, 113001 (2004)
39. E.J. Sie, T. Rohwer, C. Lee et al., Time-resolved XUV ARPES with tunable 24–33 eV laser pulses at 30 meV resolution[J]. Nat. Commun. **10**(1), 1–11 (2019)
40. M. Keunecke, C. Möller, D. Schmitt et al., Time-resolved momentum microscopy with a 1 MHz high-harmonic extreme ultraviolet beamline[J]. Rev. Sci. Instrum. **91**(6), 063905 (2020)
41. P. Miotti, F. Cilento, R. Cucini, et al., A novel high order harmonic source for time-and angle-resolved photoemission experiments[C]//compact EUV & X-ray light sources. Opt. Soc. Am. EW2B. 5 (2018)